EJN fens EUROPEAN JOURNAL OF NEUROSCIENCE

European Journal of Neuroscience, pp. 1–8, 2010 doi:10.1111/j.1460-9568.2010.07188.x

Presynaptic and postsynaptic origin of multicomponent extracellular waveforms at the endbulb of Held–spherical bushy cell synapse

Marei Typlt,[1] Martin D. Haustein,[2] Beatrice Dietz,[1] Jörn R. Steinert,[2] Mirko Witte,[1] Bernhard Englitz,[3] Ivan Milenkovic,[1] Cornelia Kopp-Scheinpflug,[1,2] Ian D. Forsythe[2] and Rudolf Rübsamen[1]

[1]Institute of Biology II, Faculty of Biosciences, Pharmacy and Psychology, University of Leipzig, Talstr. 33, 04103 Leipzig, Germany
[2]MRC Toxicology Unit, Hodgkin Building, University of Leicester, Leicester LE1 9HN, UK
[3]MPI for Mathematics in the Sciences, Inselstr. 22, 04103 Leipzig, Germany

Keywords: auditory brainstem, extracellular single-unit recordings, synaptic transmission

Abstract

Extracellular signals from the endbulb of Held–spherical bushy cell (SBC) synapse exhibit up to three component waves ('P', 'A' and 'B'). Signals lacking the third component (B) are frequently observed but as the origin of each of the components is uncertain, interpretation of this lack of B has been controversial: is it a failure to release transmitter or a failure to generate or propagate an action potential? Our aim was to determine the origin of each component. We combined single- and multiunit *in vitro* methods in Mongolian gerbils and Wistar rats and used pharmacological tools to modulate glutamate receptors or voltage-gated sodium channels. Simultaneous extra- and intracellular recordings from single SBCs demonstrated a presynaptic origin of the P-component, consistent with data obtained with multielectrode array recordings of local field potentials. The later components (A and B) correspond to the excitatory postsynaptic potential (EPSP) and action potential of the SBC, respectively. These results allow a clear interpretation of *in vivo* extracellular signals. We conclude that action potential failures occurring at the endbulb–SBC synaptic junction largely reflect failures of the EPSP to trigger an action potential and not failures of synaptic transmission. The data provide the basis for future investigation of convergence of excitatory and inhibitory inputs in modulating transmission at a fully functional neuronal system using physiological stimulation.

Introduction

The correlation of *in vivo* extracellular spike waveforms with intracellularly recorded action potentials (APs) is usually straightforward but, when orthodromic field potentials include a large presynaptic component and/or large suprathreshold synaptic component, considerable care must be taken in assigning an origin for each component. There are two well-known giant relay synapses in the auditory pathway, called the endbulb and calyx of Held, which show multi-component signal waveforms in extracellular recordings. Two extracellular components can be observed for the synaptic response at the calyx of Held in the medial nucleus of the trapezoid body (MNTB), and these can be ascribed to pre- and postsynaptic origins (Guinan & Li, 1990; Forsythe, 1994; Haustein *et al.*, 2008). However, the origin of the components in the extracellular waveforms for the endbulb of Held–spherical bushy cell (SBC) synapse has remained inconclusive.

The endbulbs of Held, which are large axosomatic synaptic terminals formed by auditory nerve fibres, provide the main excitatory input to the SBCs in the anteroventral cochlear nucleus (AVCN; Held, 1893; Brawer & Morest, 1975; Ryugo & Sento, 1991; Nicol & Walmsley, 2002). The complex waveforms obtained in extracellular recordings at endbulb–SBC synapses are composed of three components: 'P', 'A', and 'B' (Pfeiffer, 1966; Fig. 1a and b). Based on the temporal relationship between the components, Pfeiffer (1966) proposed that the initial P-component is associated with the AP in the presynaptic terminal or axon, the A-component with the excitatory postsynaptic potential (EPSP) and the B-component with the AP discharge of the SBC soma. However, alternative interpretations are: (i) the A- and B-components could relate to the initial segment AP and the backpropagating somatic–dentritic AP, respectively; or (ii) they could reflect the activity of two neighbouring SBCs, in which the AP generation might be correlated by innervation of the same auditory nerve fibre (Ryugo & Sento, 1991), gap junction connections between SBCs (Sotelo *et al.*, 1976; Gomez-Nieto & Rubio, 2009) or phase-locking to low-frequency sound.

It is important to identify the origin of each signal component to permit proper integration of *in vivo* and *in vitro* data and for interpretation of the controversial findings of transmission failures at the endbulb and calyx relay synapses *in vivo* (Pfeiffer, 1966; Bourk, 1976; Kopp-Scheinpflug *et al.*, 2002, 2003, 2008; Mc Laughlin *et al.*,

Correspondence: Marei Typlt, as above.
E-mail: typelt@uni-leipzig.de

Received 27 November 2009, revised 2 February 2010, accepted 19 February 2010

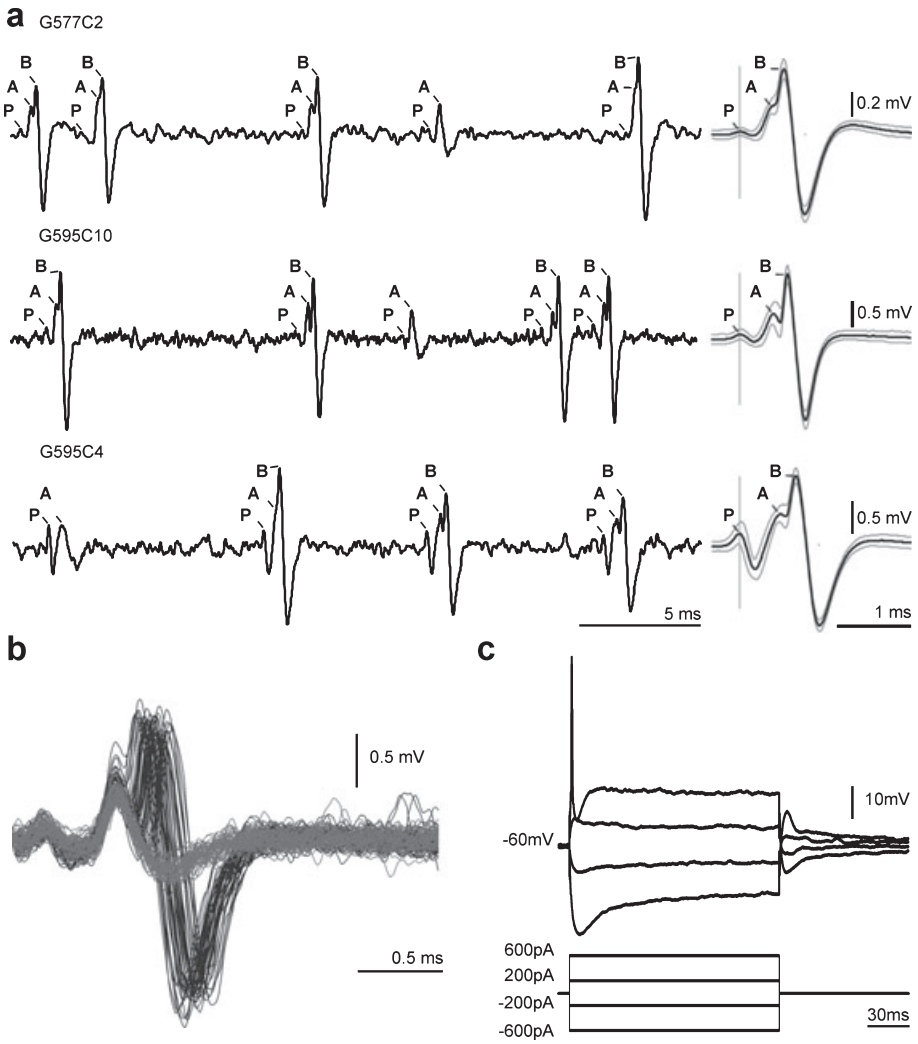

FIG. 1. *In vivo* and *in vitro* characterization of spherical bushy cells. (a) Typical unitary field potentials recorded *in vivo* from three spontaneously active SBCs of the Mongolian gerbil. Most events have three components (P, A and B), but a significant number of unitary events lack the large third component (one example in each trace). To the right of each trace, the averaged waveforms (black line) and their standard deviation (grey line) are plotted (> 1000 waveforms per average). Note that the size and delay of each wave component varies within recordings and between units. Normally, the P-component is small and hardly detectable (G577C2), but in some units it is nearly as large as the A-component (G595C4). (b) Superimposed signals of a SBC recorded *in vivo* (G595C10; second example in the upper graph), showing either all three wave components (black lines) or only the first two components (gray lines). The amplitudes and the time courses of the signals lacking the third component are the same as in the signals showing three wave components, assuming that the two types of event have a common source. (c) Current-clamp protocol to identify SBCs *in vitro* (Wistar rats). Typically, depolarizing currents evoked single or a few APs and hyperpolarizing currents evoked responses that sagged quickly.

2008; Englitz *et al.*, 2009; Lorteije *et al.*, 2009). Thus, the goal of the present study was to identify the physiological correlates of the different signal components at the endbulb of Held–SBC synapse in the AVCN. To this end, simultaneous whole-cell and extracellular recordings were obtained from SBCs, and the signal components were compared with and without application of the glutamate receptor antagonist kynurenic acid. The results confirm one of the hypotheses of Pfeiffer (1966), namely that the origin of the P-component is presynaptic, the A-component reflects the EPSP and the B-component the postsynaptic AP.

Material and methods

Simultaneous extracellular and whole-cell patch recordings were made from single SBCs in brain slices to allow direct comparison of the action potential waveforms. For further characterization of the components of the extracellular complex waveform we also made use of multielectrode array (MEA) recordings, an *in vitro* technique to record local field potentials from multiple units. This was necessary because the extracellular *in vitro* signals at single SBCs did not invariably exhibit the first component (P). Signals recorded with MEAs always show this first component which facilitates its pharmacological characterization. Additional *in vivo* recordings were acquired to aid comparison with the *in vitro* data.

Simultaneous extra- and intracellular recordings

These experiments were performed at the MRC Toxicology Unit in Leicester, UK, in accordance with the UK Animals (Scientific Procedures) Act 1986. Methods were adapted from Doughty *et al.* (1998) and Steinert *et al.* (2008). Briefly, Wistar rats aged postnatal day (P)8–P14 were killed by decapitation. Parasagittal brain slices of

the cochlear nucleus were cut (200 μm) in low-sodium aCSF at approximately 0°C. Experiments were performed at 36°C using a feedback control Peltier device warming the superfusion aCSF. Synaptic stimulation (rectangular pulses, approximately 3–8 mV, 0.1–0.2 ms, at 50 Hz for 10 s) was delivered via a bipolar platinum electrode placed at the auditory nerve fibre region using a DS2A isolated stimulator (Digitimer, Welwyn Garden City, UK). Recordings were made from visually identified neurons in the rostral AVCN, the primary location of the SBCs. Using the two-channel Multiclamp 700B amplifier (Molecular Devices, Sunnyvale, CA, USA), whole-cell patch-clamp and extracellular recordings were acquired simultaneously. Both signals were sampled at 50 kHz and low-pass filtered at 10 kHz. Recording electrodes were pulled from glass capillaries (GC150F-7.5, OD 1.5 mm; Harvard Apparatus, Edenbridge, UK). The patch pipettes had resistances of 2–5 MΩ and were filled with a pipette solution. The electrodes for the extracellular recordings had resistances between 6 and 11 MΩ and were filled with 3 M KCl. To ensure that both electrodes record from the same cell, signals were visually controlled for correlation in time and amplitude. The competitive glutamate receptor antagonist kynurenic acid (5 mM; Ganong *et al.*, 1983; Diamond & Jahr, 1997; Wong *et al.*, 2003) was applied by superfusion in the aCSF. SBCs were identified by their responses to hyper- and depolarizing current injections (Fig. 1c; Cao *et al.*, 2007; Milenkovic *et al.*, 2009). Stimulation, data acquisition and analysis were performed using commercially available software pCLAMP 9 and Clampfit 10.2 (Molecular Devices). Mean data are presented ± SEM.

Multielectrode array recordings

The following experiments were conducted at the Institute of Biology II of the University of Leipzig and were approved by the Saxonian district government Leipzig in accordance with the European Communities Council Directive (86/609/EEC).

The recording technique was adapted for AVCN from Haustein *et al.* (2008), where it was demonstrated for the MNTB that pre- and postsynaptic events could be clearly differentiated with MEA recordings. Furthermore, this technique allows the use of older animals (> P30) which were typically used for the *in vivo* studies. Briefly, slice preparation (250 μm) was the same as for single-unit recordings, but from Mongolian gerbils (*Meriones unguiculatus*) aged P40–P50. Slices were positioned with the AVCN over the electrode field and superfused with aCSF. Experiments addressing the timing between the components were conducted at near physiological temperature by heating the superfused aCSF to 32–36°C. Pharmacological experiments with the MEA were performed at room temperature, at which the recordings were more stable. Endbulb axons were stimulated (biphasic pulses, 30 μA, 80 μs/phase) with a monopolar tungsten electrode (diameter 125 μm; Science Products, Hofheim, Germany) placed in the auditory nerve region using an STG 1004 stimulus generator (Multi Channel Systems, Reutlingen, Germany). Recordings were made with arrays of 60 planar titanium nitride electrodes arranged in an 8 × 8 grid with 200 μm separation between electrodes (Multi Channel Systems). Signals were measured in reference to a bath electrode and amplified × 1200 at a sampling rate of 25 kHz, using a 60-channel MEA amplifier (MEA-1060; Multi Channel Systems). To distinguish pre- and postsynaptic components we used the AMPA/kainate receptor antagonist NBQX (10 μM) and the Na^+ channel blocker tetrodotoxin (TTX; 0.5 μM). Commercially available (MC Rack, MC Stimulus; Multi Channel Systems) and custom MATLAB (7.5.0; The Mathworks Inc., Natick, MA, USA) software were used for stimulation, data acquisition and analysis.

In vivo *recordings*

Extracellular recordings of spontaneous discharges were made from single SBCs in three adult anesthetized Mongolian gerbils (*Meriones unguiculatus*). The anaesthesia was a mixture of ketamine hydrochloride (18 mg/100 g body weight) and xylazine hydrochloride (0.7 mg/100 g body weight). Recordings were made using glass pipettes (6–11 MΩ) filled with 3 M KCl. SBCs were identified by their typical multicomponent waveform and by their response pattern to short sound stimuli. (For details see Kopp-Scheinpflug *et al.*, 2002 and Englitz *et al.*, 2009).

Composition of solutions

Artificial cerebrospinal fluid (aCSF) used for slice incubation, maintenance after slicing and superfusion during recordings contained (in mM): NaCl, 125; KCl, 2.5; $NaHCO_3$, 26; glucose, 10; NaH_2PO_4, 1.25; sodium pyruvate, 2; myo-inositol, 3; $CaCl_2$, 2; $MgCl_2$, 1; and ascorbic acid, 0.5; pH was 7.4 when gassed with 95% O_2 and 5% CO_2.

Low-sodium aCSF was used during preparation of slices, with a composition as for aCSF but NaCl was replaced by sucrose 250 mM, while $CaCl_2$ and $MgCl_2$ were changed to 0.1 and 4 mM, respectively.

The pipette solution for whole-cell recordings contained (in mM): K-gluconate, 97.5; KCl, 32.5; HEPES, 10; EGTA, 5; and $MgCl_2$, 1; pH was adjusted to 7.3 with KOH and osmolarity to 290 mOsM with sucrose.

Results

In vivo recordings from SBCs typically possess three components to their extracellular field potentials. Figure 1a shows three examples of multicomponent signals from SBCs of the Mongolian gerbil. The average traces to the right illustrate the spectrum of wave shapes (labelling of the individual components provided in the figure). Notably, the amplitude of the P-component and the delay between A and B show the largest variations across cells. Additionally, each recording shows a clear example of a failure of the B-component. In these cases, the features of the P- and A-components remain almost unchanged (Fig. 1b).

Differentiation between pre- and postsynaptic events

The first step in analysing extracellular signals was to differentiate between pre- and postsynaptic components. We obtained simultaneous extracellular and whole-cell current-clamp recordings from 14 SBCs of Wistar rats, orthodromically activated by stimulation of the auditory nerve. The extracellular *in vitro* recordings (Fig. 2b upper trace) closely matched our *in vivo* recordings (Fig 2a). The A- and B-components coincide with the intracellular postsynaptic AP (Fig. 2b, lower trace), suggesting a postsynaptic origin for both. The depicted extracellular waveforms were aligned to the P-component if P was easily discernible or otherwise to the start of the A-component. The alignment of the corresponding intracellular waveforms is constituted by the simultaneity of the intra- and extracellular recordings.

MEA recordings in the AVCN of the Mongolian gerbil following stimulation of the auditory nerve (Fig. 2c) support the hypothesis of a postsynaptic origin for the A- and B-component and additionally confirm a presynaptic origin for the P-component. These extracellular recordings are composed of two components, similar to MEA recordings from the MNTB (Haustein *et al.*, 2008): a P-wave and combined A/B-wave with a peak-to-peak latency of 0.61 ± 0.01 ms (Fig. 2c; n = 105 electrodes and 35 slices). The respective waveforms

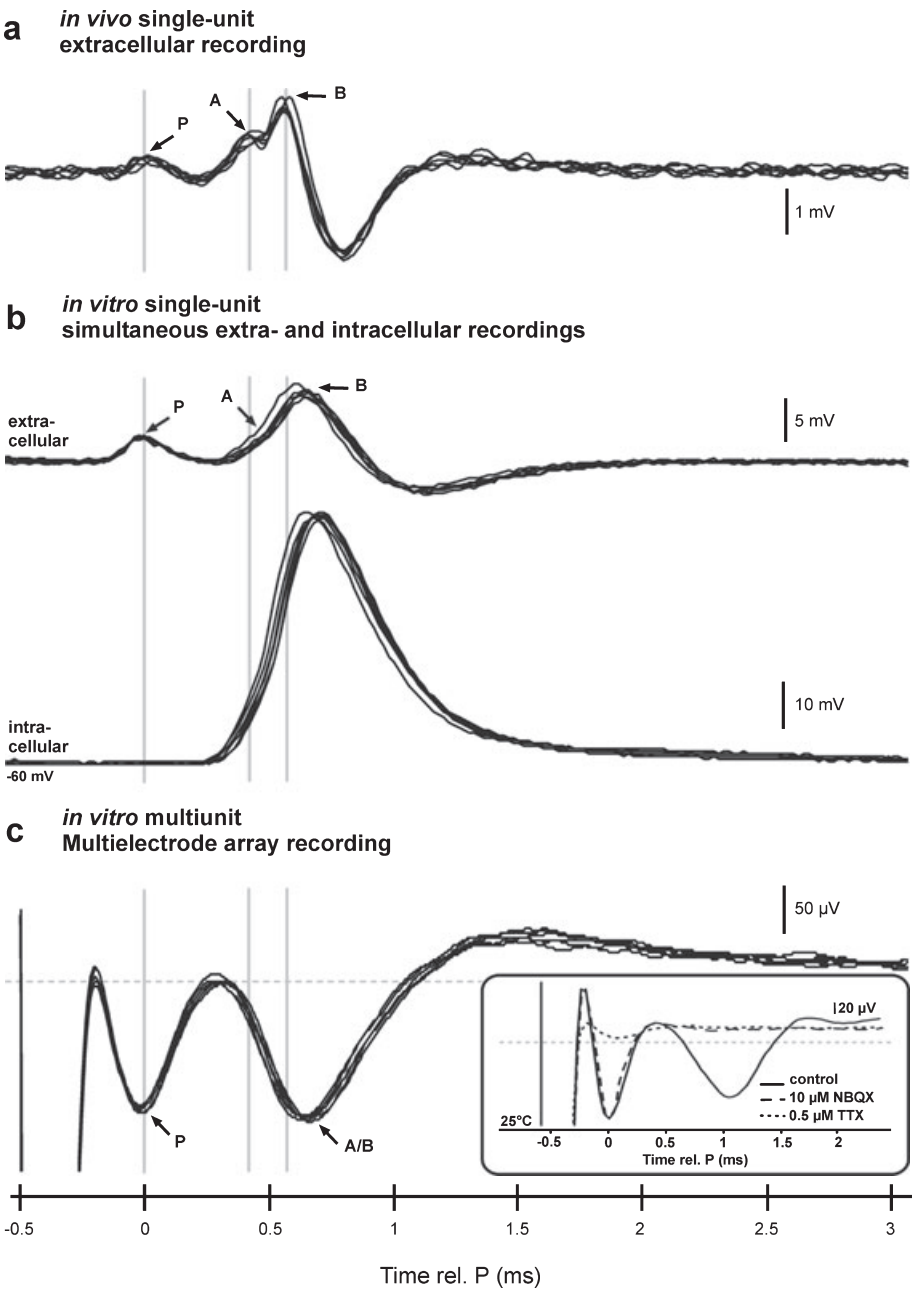

FIG. 2. Different recording techniques at the endbulb of Held–SBC synapse yielded compound waveforms with corresponding temporal properties. (a) Extracellular signals recorded *in vivo* from a SBC in the Mongolian gerbil. Five traces are superimposed and aligned to the peak of the P-component. The waveforms consist of three components with average delays of approximately 0.5 ms between P and A, and 0.2 ms between A and B. (b) Simultaneous extracellular (upper traces) and whole-cell recordings (lower traces) from an endbulb of Held–SBC synapse in a parasagittal brain slice of the AVCN of a Wistar rat at physiological temperature. SBCs were stimulated orthodromically by triggering APs in the auditory nerve (stimulus artefacts were outside the displayed time window). Five traces are superimposed, aligned to the extracellular P-component. P precedes the intracellular AP by approximately 0.7 ms. The intracellular AP then coincides with the extracellular A- and B-components, suggesting that both are of postsynaptic origin. (c) Multielectrode array recordings from the AVCN of the Mongolian gerbil (slice preparation as in b). Local field potentials were acquired from the rostral pole of the AVCN, while stimulation was applied to the auditory nerve trunk (stimulus artefacts were cut off for clarity). Dotted horizontal line indicates the base line of the recordings. Five traces are superimposed and aligned to the maximum of the first component. Classification of the components as P and A/B was based on their timing and pharmacological results (in separate experiments, at 25°C; see inset). Superfusion with NBQX had no effect on the P-wave but blocked the A/B-wave. TTX blocked P- and A/B-waves. Grey vertical lines indicate the timing of the three signal components in the *in vivo* recordings.

in Fig. 2c were aligned to their P-component. For visual comparison with the extracellular single-unit recordings in Fig. 2a and b, the P-components of all these recordings were aligned.

We used the AMPA/kainate receptor antagonist NBQX (10 μM) and the Na^+ channel blocker TTX (0.5 μM) to distinguish pre- and postsynaptic components. The A/B-wave was blocked by NBQX ($-96.1 \pm 0.1\%$, $n = 26$ electrodes in 13 slices; $P < 0.001$, rank-sum test), while the P-wave remained unchanged ($-1.1 \pm 0.8\%$, $n = 26$ electrodes in 13 slices; $P = 0.371$, rank-sum test; Fig. 2c inset, dashed line). The neuronal origin of P was shown by the application of TTX (0.5 μM), which largely abolished the P-wave ($-94.1 \pm 0.2\%$, $n = 20$ electrodes in seven slices; $P < 0.001$, *t*-test; Fig. 2c inset,

dotted line). These data indicate a presynaptic origin for P and a postsynaptic origin for A and B.

The similar temporal relationship of the signal components obtained by the use of the different extracellular recording methods (Fig. 2) suggests the same source for the respective components independent of the recording methods. Consequently, the origins of the P- and A/B-waves in the MEA recordings imply a presynaptic origin for P and a postsynaptic origin for A and B also in the single-unit recordings. However, the differentiation between the postsynaptic components A and B still remains unclear.

Differentiation between the postsynaptic A- and B-components

To understand the origins of the A- and B-components, we again compared the simultaneous extra- and intracellular single-unit recordings. Figure 3 shows paired data from two different units of Wistar rats; the respective upper traces show the extracellular recording and the lower traces the intracellular recording (simultaneously recorded signals are indicated by identical colours; alignment was the same as described for Fig. 2). In our sample of units ($n = 13$), the A-component in the extracellular signal was always significantly smaller in amplitude than the B-component (43.1 ± 5.9%; $P < 0.001$, signed-rank test). The average delay between A and B was 0.25 ± 0.03 ms ($n = 13$ units). In Fig. 3b the control (predrug) traces of the intracellular recording show the occasional failure of the postsynaptic AP, revealing the underlying EPSP. The postsynaptic components of the corresponding extracellular signal strongly co-vary with the intracellular signal. Basically, the A-component of the extracellularly recorded signal resembles a down-scaled intracellularly recorded EPSPs, suggesting that A corresponds to the EPSP of the SBC while the B is the postsynaptic AP.

This hypothesis was tested by suppression of the synaptic response by superfusion of the nonspecific glutamate receptor antagonist kynurenic acid ($n = 6$ units; Fig. 3). Initially, the time from the stimulus to the peak of the A-component increased (from 0.47 ± 0.06 to 0.63 ± 0.07 ms; $P < 0.01$, paired Wilcoxon signed-rank test). The delay between A and B also increased (from 0.26 ± 0.05 to 0.78 ± 0.30 ms; $P < 0.05$, paired Wilcoxon signed-rank test). Then, after 1–2 min the number of AP failures increased (from 54 ± 13 to 98 ± 1%; $P < 0.05$, paired Wilcoxon signed-rank test), with each failure coinciding with the absence of the B-component in the extracellular recording (Fig. 3, kynurenic acid, 2 min). Concurrently, EPSP amplitudes decreased (from 18.8 ± 2.6 to 13.5 ± 2.2 mV after 1–2 min; $P < 0.01$, paired Wilcoxon signed-rank test) and were nearly abolished (3.0 ± 1.1 mV) after 3–4 min, which corresponded to a parallel reduction in the A-component amplitude in the extracellular recording (Fig. 3, kynurenic acid, 3 min). During washout of kynurenic acid a reverse sequence of the respective changes in the intracellular and extracellular recordings was observed (Fig. 3, recovery). These results support the conclusion that the A-component of the extracellular SBC recordings corresponds to the EPSP and the B-component to the somatic AP.

Discussion

This study demonstrates that the components of extracellular field potentials from SBCs can be specifically related to intracellular events and resolves the long-standing controversy over the origin of the different wave components. We confirm that the P-component is presynaptic and that the A-component reflects the EPSP, while the B-component results from the AP of the SBC. These results allow a clear interpretation of extracellular *in vivo* recordings in the AVCN from past and future studies, and permit more advanced physiological questions relating to synaptic transmission and integration to be addressed *in vivo*.

Comparability of signals obtained with different methods

Typical *in vivo* extracellular recordings at the SBCs are described as consisting of three components with numerous events lacking the last component (Pfeiffer, 1966; Bourk, 1976; Kopp-Scheinpflug *et al.*, 2002; Stasiak *et al.*, 2008; Englitz *et al.*, 2009). Interpretation of these recordings requires comparison with intracellular recordings in order to define the underlying physiological basis of each wave component. For this purpose we combined extracellular and intracellular recording techniques *in vivo* and *in vitro*.

The timing of the respective wave components was consistent across the recording techniques, the animals and the ages that were employed (Fig. 2). We used two rodent species in this study: Mongolian gerbils and Wistar rats. For the latter no extracellular waveforms have so far been obtained from the SBC *in vivo*. However, in previous studies interspecies differences were found to be only minor (gerbil, Kopp-Scheinpflug *et al.*, 2002; Englitz *et al.*, 2009; guinea pig, Stasiak *et al.*, 2008; cat, Pfeiffer, 1966; Bourk, 1976), suggesting similarly minor differences for the present two rodent species. Further, we did not observe differences in the timing of wave components throughout a range of ages, although developmental changes at the endbulb synapses can occur up to P50 (Bellingham *et al.*, 1998; Limb & Ryugo, 2000).

While typically the postsynaptic single-unit extracellular signals consist of two clearly separated components, in some units signals with nonseparable postsynaptic components also occurred. Such fusion of A and B could be due to a fast rise time of the EPSP and a short delay in AP initiation. Still, failures of AP initiation (only EPSP remains) can be clearly distinguished from successful AP initiation (EPSP plus AP) by the larger signal amplitude in the latter case. Also, signals reflecting an AP have their peak at a longer delay after the P-component. For MEA recordings, the lack of a clear distinction between the A- and B-components is a direct consequence of summed activity from multiple units, each contributing to the local field potential (multiunit recording), but with slightly different latencies, so the total signal is smoothed and individual components are indiscernible.

Differences in the polarity between different approaches are probably due to differences in the relative locations of the electrode, presynaptic axon and postsynaptic neuron. All components of the unitary extracellular signals in this study show a positive polarity as previously described by Kopp-Scheinpflug *et al.* (2002) and Englitz *et al.* (2009). This contrasts with Pfeiffer (1966) who showed positive presynaptic components and negative postsynaptic components. Bourk (1976) recorded both positive and negative postsynaptic components. The MEA recordings show negative potentials for both presynaptic and postsynaptic components. Polarity reversal is common in studies measuring local field potentials, and several studies have addressed this question experimentally (Lorente de No, 1947; Henze *et al.*, 2000) and theoretically (Humphrey & Schmidt, 1990; Holt & Koch, 1999; Gold *et al.*, 2006). Together, these studies show that the polarity strongly depends on the location of the electrode tip relative to the recorded neuron, the anatomy of the neuron, and the distribution of current-generating regions within the neuron.

The shape of the extracellular signals is also influenced by the distance of the electrode tip from the neuronal membrane (Freygang & Frank, 1959; Holt & Koch, 1999; Henze *et al.*, 2000; Gold *et al.*,

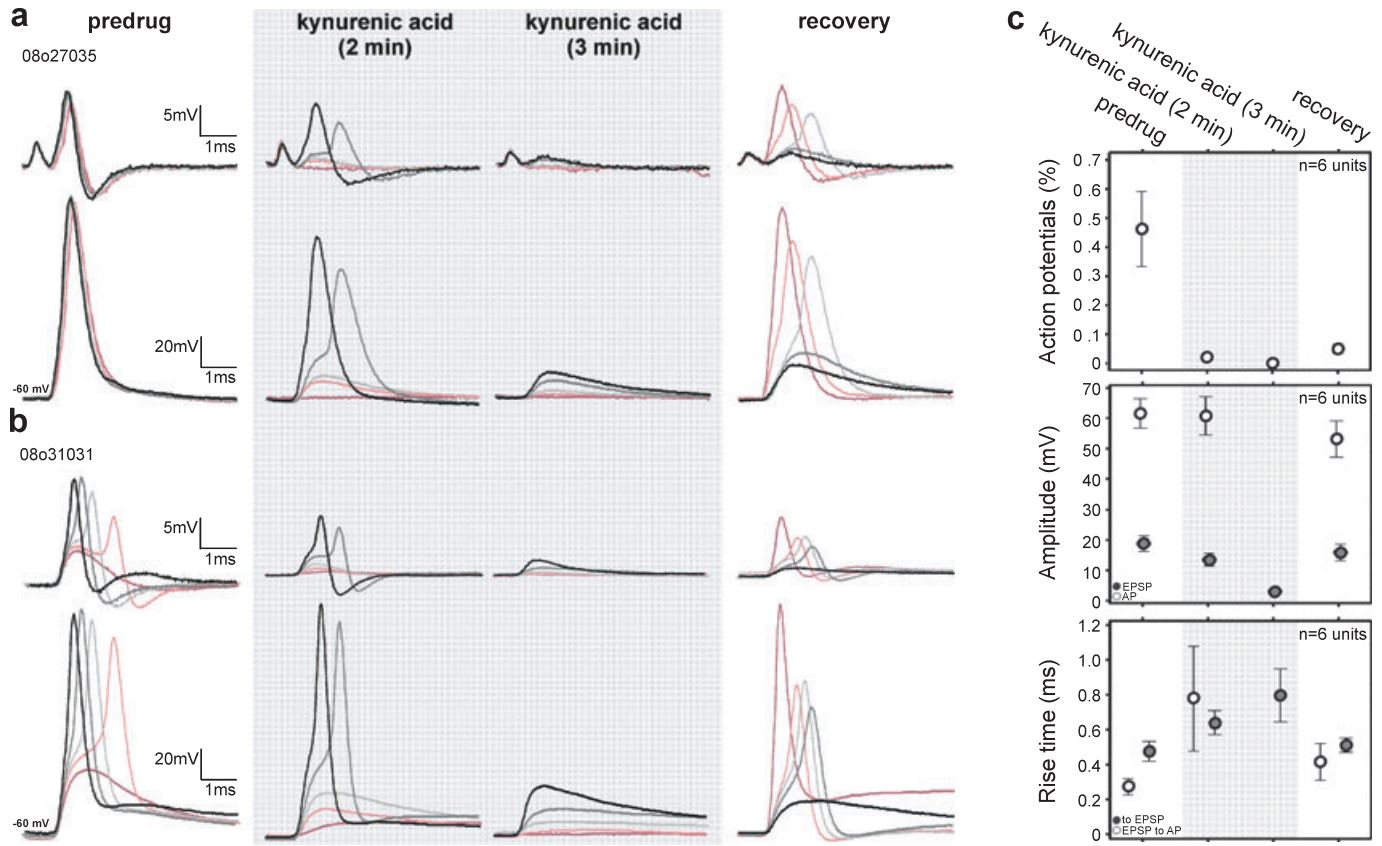

FIG. 3. Paired extra- and intracellular recordings show that the P-component was presynaptic, the A-component was the EPSP and the B-component the postsynaptic AP. Responses of SBCs of Wistar rats to electrical stimulation of auditory nerve fibres (stimulus artefacts are outside the displayed time window; each record shows five superimposed traces). (a and b) Data from different units: simultaneous extracellular (upper traces) and whole-cell patch-clamp (lower traces) recordings obtained during superfusion with aCSF (left), during application of 5 mM kynurenic acid (center, after 2 and 3 min), and recovery (right). Matching extra- and intracellularly recorded signals are indicated by identical colours (colours indicate increasing time from black to red). (a) Unit in which all three components (P, A, and B) can be distinguished in the extracellular waveform. (b) Unit showing a wider variation in delay between the two postsynaptic signal components in the predrug condition. Here, in the predrug condition initially the two postsynaptic components were not separable. With ongoing stimulation, the delay increased, the A-component became more prominent and occasionally the B-component was missing. Bath application of kynurenic acid (2 min) progressively antagonized the postsynaptic action of glutamate, which was reflected in the increase in delay between P, A and B. After the complete block of the B-component (3 min), the A-component also gradually decreased until it was abolished. Both the A- and B-component gradually recovered during the washout (right panel, black to red, 2–10 min from the beginning of the washout). The P-component (in a) was only slightly affected, indicating its presynaptic nature. The successive block of the A- and B-components together with the respective changes in the intracellularly recorded voltages suggest that the A-component is the extracellularly recorded EPSP and the B-component the AP of the SBC. (c) Population analyses (n = 6 units, means ± SEM) of the probability of occurrence of APs (top), the amplitude (middle), and the temporal characteristics (bottom) of the signal components under the different conditions.

2006). A far field recording will reflect the capacitative current across the membrane which corresponds to the derivative of the membrane potential, while an electrode which directly contacts the membrane forming a high ohmic seal will pick up a scaled version of the transmembrane potential (corresponding to a non-ruptured patch recording). In practice, each *in vivo* and *in vitro* extracellular recording will be between these two extremes, and the recorded signal will be a mixture of both (i.e. the derivative of the transmembrane voltage and the transmembrane voltage itself). Responses to postsynaptic current injections (data not shown) support this theory: the extracellular signals are similar in shape to the whole-cell recordings, yet feature relatively increased amplitudes at times when the intracellular voltage changes sharply (thus agreeing with the contribution of the derivative). However, the derivative cannot be the only contribution, as the extracellular signal retains a slowly varying component (thus agreeing with the direct contribution of the intracellular voltage). The recent study from Lorteije *et al.* (2009) presented a similar interpretation for simultaneous recordings in the MNTB which was substantiated by a compartmental model of the translation from intracellular to extracellular potential. The differences obtained between the present extracellular *in vitro* and *in vivo* recordings can be explained in agreement with this interpretation and the attribution of the different components remains valid.

Concerning the comparison of extra- and intracellular recordings, this interpretation would furthermore explain the more prominent negative deflection at the end of the AP and the temporal shift between the intra- and the extracellular AP peak. Another difference between extra- and intracellular recordings, i.e. the absence of the P-component in the intracellular recordings, can be explained by electrical compartmentalization between the pre- and postsynaptic sites (Forsythe, 1994).

Alternative hypotheses

The alternative hypotheses for the origins of the three wave components are not supported by our experiments. The simultaneous extra- and intracellular recordings reveal that the A-component is not an AP generated at the axon hillock, nor is the B-component a

backpropagating AP as suggested by Pfeiffer (1966), as, in this case, the glutamate receptor antagonist kynurenic acid should have extinguished both components simultaneously. Kynurenic acid does not block backpropagating APs, therefore signals consisting exclusively of P- and A-components should not occur if this hypothesis holds. The graded nature of the A-component excludes the possibility that A is an all-or-nothing AP generated at the axon hillock. Furthermore, the A- and B-components cannot reflect the APs of neighbouring cells, as then B should occasionally occur without a preceding P and A. In addition, both recorded cells should be simultaneously affected by kynurenic acid. Neither phenomenon was ever observed.

Lorteije *et al.* (2009) also used simultaneous extra- and intracellular recordings to address a similar question at the calyx of Held in the MNTB. Guinan & Li (1990) and Haustein *et al.* (2008) have previously shown that the extracellular recording reflects both pre- and postsynaptic activity. Lorteije *et al.* (2009) concluded that the postsynaptic activity is composed of the EPSP and AP activity, which is similar to our results in the AVCN.

In both the AVCN and MNTB nuclei, the different extracellularly recorded signal components mutually influence each other with respect to signal shape and dynamics. In particular, the two postsynaptic components, A and B, interfere due to their temporal adjacency. For the present approach detecting the respective components was sufficient, but for quantitative measurements in future studies, considerable care must be taken concerning this issue. Despite this problem Lorteije *et al.* (2009) showed that the extracellular signals could also be used to estimate presynaptic release and postsynaptic excitability in the MNTB.

Action potential failures

Several studies have already provided evidence for failures of AP transmission at the SBC in response to input from the endbulbs (*in vivo*: Pfeiffer, 1966; Bourk, 1976; Kopp-Scheinpflug *et al.*, 2002; Englitz *et al.*, 2009; *in vitro*: Oertel, 1983; Wang & Manis, 2006). Theoretically, these failures could have pre- or postsynaptic causes. From the present study we conclude that AP failures are largely due to the failure of the EPSP to generate a postsynaptic AP. However, we cannot exclude the possibility of failures of the presynaptic input to trigger an EPSP.

The functional significance of these AP failures has been linked to the parallel observation of a sharpened frequency tuning (Kopp-Scheinpflug *et al.*, 2002) and a temporal sharpening in phase-locking (Dehmel *et al.*, 2005) from the presynaptic input to the postsynaptic output of the SBCs. Summation of multiple excitatory endbulb inputs (Rothman *et al.*, 1993; Joris *et al.*, 1994; Rothman & Young, 1996; Kuhlmann *et al.*, 2002; Xu-Friedman & Regehr, 2005a,b; Yang & Xu-Friedman, 2009) and inhibitory inputs (Kopp-Scheinpflug *et al.*, 2002) could underlie this temporal processing.

Conclusion

The assignment of the different components of extracellularly recorded signals of the endbulb of Held–SCB synapse to specific intracellular electric events will enable the investigation of developmental and activity dependent factors affecting the reliability of synaptic transmission and integration. Such studies can be performed in an intact neuronal system using systemic acoustic stimulation. Furthermore, comparison with data from the calyx of Held will open the possibility of interpreting the data in the context of different synaptic properties such as the size of the synapse and number of converging inputs.

Acknowledgements

This work was supported by the DAAD (D/08/44134), the DFG (Ru390-18/1, Mi954-1/2) and the MRC (UK). The authors additionally benefit from the Graduate College InterNeuro at the University Leipzig (DFG GRK 1097) and the Research Academy Leipzig. M.D.H. was funded by a PhD Scholarship from Deafness Research UK.

Abbreviations

aCSF, artificial cerebrospinal fluid; AP, action potential; AVCN, anteroventral cochlear nucleus; EPSP, excitatory postsynaptic potential; MEA, multielectrode array; MNTB, medial nucleus of trapezoid body; P, postnatal day; SBC, spherical bushy cell; TTX, tetrodotoxin.

References

Bellingham, M.C., Lim, R. & Walmsley, B. (1998) Developmental changes in EPSC quantal size and quantal content at a central glutamatergic synapse in rat. *J. Physiol.*, **511**(Pt 3), 861–869.

Bourk, T. (1976) *Electrical Responses of Neuronal Units in the Anteroventral Cochlear Nucleus of the Cat*. Dissertation, Massachusetts Institute of Technology, Cambridge.

Brawer, J.R. & Morest, D.K. (1975) Relations between auditory nerve endings and cell types in the cat's anteroventral cochlear nucleus seen with the Golgi method and Nomarski optics. *J. Comp. Neurol.*, **160**, 491–506.

Cao, X.J., Shatadal, S. & Oertel, D. (2007) Voltage-sensitive conductances of bushy cells of the Mammalian ventral cochlear nucleus. *J. Neurophysiol.*, **97**, 3961–3975.

Dehmel, S., Kopp-Scheinpflug, C. & Rubsamen, R. (2005) Interplay of excitation and inhibition in auditory brainstem processing at endbulbs of held of the MNTB and AVCN *4th Conference on Plasticity of the Central Auditory System and Processing of Complex Acoustic Signals*, Prague, pp. 15–36.

Diamond, J.S. & Jahr, C.E. (1997) Transporters buffer synaptically released glutamate on a submillisecond time scale. *J. Neurosci.*, **17**, 4672–4687.

Doughty, J.M., Barnes-Davies, M., Rusznak, Z., Harasztosi, C. & Forsythe, I.D. (1998) Contrasting Ca^{2+} channel subtypes at cell bodies and synaptic terminals of rat anterioventral cochlear bushy neurones. *J. Physiol.*, **512** (Pt 2), 365–376.

Englitz, B., Tolnai, S., Typlt, M., Jost, J. & Rubsamen, R. (2009) Reliability of synaptic transmission at the synapses of Held in vivo under acoustic stimulation. *PLoS ONE*, **4**(10), e7014.

Forsythe, I.D. (1994) Direct patch recording from identified presynaptic terminals mediating glutamatergic EPSCs in the rat CNS, in vitro. *J. Physiol.*, **479**(Pt 3), 381–387.

Freygang, W.H. Jr & Frank, K. (1959) Extracellular potentials from single spinal motoneurons. *J. Gen. Physiol.*, **42**, 749–760.

Ganong, A.H., Lanthorn, T.H. & Cotman, C.W. (1983) Kynurenic acid inhibits synaptic and acidic amino acid-induced responses in the rat hippocampus and spinal cord. *Brain Res.*, **273**, 170–174.

Gold, C., Henze, D.A., Koch, C. & Buzsaki, G. (2006) On the origin of the extracellular action potential waveform: a modeling study. *J. Neurophysiol.*, **95**, 3113–3128.

Gomez-Nieto, R. & Rubio, M.E. (2009) A bushy cell network in the rat ventral cochlear nucleus. *J. Comp. Neurol.*, **516**, 241–263.

Guinan, J.J. Jr & Li, R.Y. (1990) Signal processing in brainstem auditory neurons which receive giant endings (calyces of Held) in the medial nucleus of the trapezoid body of the cat. *Hear. Res.*, **49**, 321–334.

Haustein, M.D., Reinert, T., Warnatsch, A., Englitz, B., Dietz, B., Robitzki, A., Rubsamen, R. & Milenkovic, I. (2008) Synaptic transmission and short-term plasticity at the calyx of Held synapse revealed by multielectrode array recordings. *J. Neurosci. Methods*, **174**, 227–236.

Held, H. (1893) Die zentrale Gehörleitung. In His, W. & Bois-Reymond, E.D. (Eds), *Archiv für Anatomie und Physiologie*. Leipziger Verlag von Veit und Comp, Leipzig, pp. 201–248.

Henze, D.A., Borhegyi, Z., Csicsvari, J., Mamiya, A., Harris, K.D. & Buzsaki, G. (2000) Intracellular features predicted by extracellular recordings in the hippocampus in vivo. *J. Neurophysiol.*, **84**, 390–400.

Holt, G.R. & Koch, C. (1999) Electrical interactions via the extracellular potential near cell bodies. *J. Comput. Neurosci.*, **6**, 169–184.

Humphrey, D.R. & Schmidt, E.M. (1990) Extracellular Single-Unit Recording Methods. In Boulton, A.A., Baker, G.B. & Vanderwolf, C.H. (Eds), *Neuromethods*, Vol. **15**. The Humana Press Inc, Clifton, pp 1–64.

Joris, P.X., Carney, L.H., Smith, P.H. & Yin, T.C. (1994) Enhancement of neural synchronization in the anteroventral cochlear nucleus. I. Responses to tones at the characteristic frequency. *J. Neurophysiol.*, **71**, 1022–1036.

Kopp-Scheinpflug, C., Dehmel, S., Dorrscheidt, G.J. & Rubsamen, R. (2002) Interaction of excitation and inhibition in anteroventral cochlear nucleus neurons that receive large endbulb synaptic endings. *J. Neurosci.*, **22**, 11004–11018.

Kopp-Scheinpflug, C., Lippe, W.R., Dorrscheidt, G.J. & Rubsamen, R. (2003) The medial nucleus of the trapezoid body in the gerbil is more than a relay: comparison of pre- and postsynaptic activity. *J. Assoc. Res. Otolaryngol.*, **4**, 1–23.

Kopp-Scheinpflug, C., Dehmel, S., Tolnai, S., Dietz, B., Milenkovic, I. & Rubsamen, R. (2008) Glycine-mediated changes of onset reliability at a mammalian central synapse. *Neuroscience*, **157**, 432–445.

Kuhlmann, L., Burkitt, A.N., Paolini, A. & Clark, G.M. (2002) Summation of spatiotemporal input patterns in leaky integrate-and-fire neurons: application to neurons in the cochlear nucleus receiving converging auditory nerve fiber input. *J. Comput. Neurosci.*, **12**, 55–73.

Limb, C.J. & Ryugo, D.K. (2000) Development of primary axosomatic endings in the anteroventral cochlear nucleus of mice. *J. Assoc. Res. Otolaryngol.*, **1**, 103–119.

Lorente de No, R. (1947) A study of nerve physiology. *Stud. Rockefeller. Inst. Med. Res. Repr.*, **131**, 132.

Lorteije, J.A., Rusu, S.I., Kushmerick, C. & Borst, J.G. (2009) Reliability and precision of the mouse calyx of Held synapse. *J. Neurosci.*, **29**, 13770–13784.

Mc Laughlin, M., van der Heijden, M. & Joris, P.X. (2008) How secure is in vivo synaptic transmission at the calyx of Held? *J. Neurosci.*, **28**, 10206–10219.

Milenkovic, I., Rinke, I., Witte, M., Dietz, B. & Rubsamen, R. (2009) P2 receptor-mediated signaling in spherical bushy cells of the mammalian cochlear nucleus. *J. Neurophysiol.*, **102**, 1821–1833.

Nicol, M.J. & Walmsley, B. (2002) Ultrastructural basis of synaptic transmission between endbulbs of Held and bushy cells in the rat cochlear nucleus. *J. Physiol.*, **539**, 713–723.

Oertel, D. (1983) Synaptic responses and electrical properties of cells in brain slices of the mouse anteroventral cochlear nucleus. *J. Neurosci.*, **3**, 2043–2053.

Pfeiffer, R.R. (1966) Anteroventral cochlear nucleus: wave forms of extracellularly recorded spike potentials. *Science*, **154**, 667–668.

Rothman, J.S. & Young, E.D. (1996) Enhancement of neural synchronization in computational models of cochlear nucleus bushy cells. *Aud. Neurosci.*, **2**, 47–62.

Rothman, J.S., Young, E.D. & Manis, P.B. (1993) Convergence of auditory nerve fibers onto bushy cells in the ventral cochlear nucleus: implications of a computational model. *J. Neurophysiol.*, **70**, 2562–2583.

Ryugo, D.K. & Sento, S. (1991) Synaptic connections of the auditory nerve in cats: relationship between endbulbs of held and spherical bushy cells. *J. Comp. Neurol.*, **305**, 35–48.

Sotelo, C., Gentschev, T. & Zamora, A.J. (1976) Gap junctions in ventral cochlear nucleus of the rat. A possible new example of electrotonic junctions in the mammalian C.N.S. *Neuroscience*, **1**, 5–7.

Stasiak, A., Sayles, M. & Winter, I. (2008) Spike Waveforms in the Anteroventral Cochlear Nucleus Revisited. *31th annual Midwinter Research Meeting of the ARO*. Assoc. Res. Otolaryngol., Phoenix, pp. 279–280.

Steinert, J.R., Kopp-Scheinpflug, C., Baker, C., Challiss, R.A., Mistry, R., Haustein, M.D., Griffin, S.J., Tong, H., Graham, B.P. & Forsythe, I.D. (2008) Nitric oxide is a volume transmitter regulating postsynaptic excitability at a glutamatergic synapse. *Neuron*, **60**, 642–656.

Wang, Y. & Manis, P.B. (2006) Temporal coding by cochlear nucleus bushy cells in DBA/2J mice with early onset hearing loss. *J. Assoc. Res. Otolaryngol.*, **7**, 412–424.

Wong, A.Y., Graham, B.P., Billups, B. & Forsythe, I.D. (2003) Distinguishing between presynaptic and postsynaptic mechanisms of short-term depression during action potential trains. *J. Neurosci.*, **23**, 4868–4877.

Xu-Friedman, M.A. & Regehr, W.G. (2005a) Dynamic-clamp analysis of the effects of convergence on spike timing. I. Many synaptic inputs. *J. Neurophysiol.*, **94**, 2512–2525.

Xu-Friedman, M.A. & Regehr, W.G. (2005b) Dynamic-clamp analysis of the effects of convergence on spike timing. II. Few synaptic inputs. *J. Neurophysiol.*, **94**, 2526–2534.

Yang, H. & Xu-Friedman, M.A. (2009) Impact of synaptic depression on spike timing at the endbulb of held. *J. Neurophysiol.*, **102**, 1699–1710.